Time-resolved Electron Microscopic Analysis of the Behavior of Myosin Heads on Actin Filaments after Photolysis of Caged ATP

Takashi Funatsu,* Eiji Kono,*‡ and Shoichiro Tsukita*

*Department of Information Physiology, National Institute for Physiological Sciences, Myodaiji, Aichi 444, Japan; and
‡Molecular Electronics Laboratory, Tsukuba Research Center, SANYO Electric Co. Ltd., Koyadai, Ibaraki 305, Japan

Abstract. The interaction between myosin subfragment 1 (S1) and actin filaments after the photolysis of P^3-1-(2-nitrophenyl)ethyl ester of ATP (caged ATP) was analyzed with a newly developed freezing system using liquid helium. Actin and S1 (100 μM each) formed a ropelike double-helix characteristic of rigor in the presence of 5 mM caged ATP at room temperature. At 15 ms after photolysis, the ropelike double helix was partially disintegrated. The number of S1 attached to actin filaments gradually decreased up to 35 ms after photolysis, and no more changes were detected from 35 to 200 ms. After depletion of ATP, the ropelike double helix was reformed. Taking recent analyses of actomyosin kinetics into consideration, we concluded that most S1 observed on actin filaments at 35–200 ms are so called "weakly bound S1" (S1.ATP or S1.ADP.Pi) and that the weakly bound S1 under a rapid association–dissociation equilibrium with actin filaments can be captured by electron microscopy by means of our newly developed freezing system.

This enabled us to directly compare the conformation of weakly and strongly bound S1. Within the resolution of deep-etch replica technique, there were no significant conformational differences between weakly and strongly bound S1, and neither types of S1 showed any positive cooperativity in their binding to actin filaments. Close comparison revealed that the weakly and strongly bound S1 have different angles of attachment to actin filaments. As compared to strongly bound S1, weakly bound S1 showed a significantly broader distribution of attachment angles. These results are discussed with special reference to the molecular mechanism of acto–myosin interaction in the presence of ATP.

MUSCLE contracts by the interaction of myosin cross-bridges with actin filaments using chemical energy from ATP hydrolysis. Biochemical studies of actomyosin solutions have suggested that myosin heads bound to actin filaments take two distinct conformations, strongly and weakly bound, and that the respective conformations correspond to actin.S1.ADP/actin.S1 and actin.S1.ATP/actin.S1.ADP.Pi (Eisenberg and Hill, 1985). Experimental evidence for the existence of the weakly bound cross-bridge state in muscles has accumulated (Matsuda and Podolsky, 1984; Brenner et al., 1982, 1984). X-ray diffraction patterns of living muscle have suggested that myosin heads are in close proximity to actin filaments during contraction (Haselgrove and Huxley, 1973) and that weakly bound cross-bridges have a wide range of permitted orientations and are in rapid equilibrium of attachment to and detachment from actin filaments (Huxley and Kress, 1985).

It has become necessary to directly visualize the myosin heads (myosin subfragment 1; S1)[1] which interact with actin filaments in the presence of ATP. Since recent progress in rapid freezing EM has greatly improved the temporal resolution of images (Heuser et al., 1979), EM should provide the most direct information on the conformation of weakly bound cross-bridges. Tsukita and Yano (1985, 1988) analyzed images from thin sections of freeze-substituted rabbit skeletal muscle rapidly frozen during isometric contraction or free shortening, and concluded that the cross-bridge configuration during contraction is distinct from that in rigor.

To understand the behavior of the weakly bound myosin head in more detail using EM, the S1 molecules which interact with actin filaments in vitro in the presence of ATP need to be observed. However, for this type of observation, a high concentration of actin and S1 is required because of the low affinity of the weakly bound S1 for actin filaments (Stein et al., 1979; Chalovich and Eisenberg, 1981), which generally interferes with electron microscopic observations. Craig et al. (1985) and Applegate and Flicker (1987) tried to circumvent this issue in negative staining or frozen-hydrated EM by means of S1 chemically cross-linked to actin filaments. In both reports, however, the possibility could not be ruled out that some population of S1 observed on actin filaments were

T. Funatsu's present address is Yanagida Biomotron Project, Exploratory Research for Advanced Technology, Research Development Corporation of Japan, 2-4-14 Senba-higashi, Mino, Osaka 562, Japan.

1. *Abbreviations used in this paper:* S1, myosin subfragment 1; caged ATP, P^3-1-(2-nitrophenyl)ethyl ester of ATP; TES, *N*-Tris (hydroxymethyl) methyl-2-aminoethanesulphonic acid.

merely tethered to actin filaments by chemical cross-linkers. Recently, Frado and Craig (1992) tried to improve the temporal resolution of negative staining and concluded that the configuration of acto-heavy-meromyosin in the presence of ATP is distinct from that in rigor. Katayama (1989) applied the mica-flake method combined with quick freezing using intact actin–S1 complexes in the presence of ATP. However, the concentration of actin–S1 that he used was quite low (~10 μM of actin and S1 in 70 mM KCl), which made the number of weakly bound S1 very small. A higher concentration of actin-S1 would interfere with observations of weakly bound S1 by large amounts of it being absorbed on the mica and by the depletion of ATP during preparation. As another type of application of quick-freeze technique in this field, Pollard et al. (1990) have recently developed a stopped-flow/rapid-freezing machine.

We have developed a new rapid-freezing system which permits the photolysis of caged ATP in the sample just before freezing. The photolysis of caged ATP enabled us to abruptly increase the concentration of ATP in the sample without diffusion delay (McCray et al., 1980). By combining this system with the deep-etch replica method (Heuser, 1981), high concentrations of actin and S1 can be analyzed with the electron microscope: the abrupt increase of the ATP concentration just before freezing relieves the problem of ATP depletion, and fracturing the sample before etching allows observation of the actin-bound S1 without the interference of a large number of free S1. In this study, by applying a high concentration of the fully decorated actin–S1 containing caged ATP to our newly developed freezing system, we analyzed the behavior of S1 on actin filaments after photolysis of caged ATP and concluded that the weakly bound S1 under rapid association–dissociation equilibrium with actin filaments can be captured by EM in vitro. Using this system combined with the deep-etch replica technique, we compared the conformation of weakly bound S1 with that of strongly bound S1, focussing upon the angle and cooperativity in the binding of S1 to actin filaments.

Materials and Methods

Chemicals

Caged ATP purchased from Dojindo Lab. (Kumamoto, Japan) contained <0.03% of contaminating ATP as determined using a luciferin–luciferase assay kit (ATP bioluminescence CLS; Boehringer Mannheim Biochemical, Indianapolis, IN).

Samples for Rapid Freezing

Muscle proteins were prepared from rabbit leg and back white muscle. Actin was extracted from an acetone powder and purified according to the method developed by Spudich and Watt (1971). Chymotryptic S1 was prepared by the method of Weeds and Taylor (1975), and S1(A1) was used to avoid possible artifacts due to isoenzymes. The concentrations of proteins were determined by the biuret method or by a dye-binding assay (Bradford, 1976) calibrated by extinction coefficients at 280 nm (White and Taylor, 1976). Actin-activated ATPase activity of the S1 preparations we used was measured with increasing concentrations of actin in the presence of 5 mM ATP, 20 mM KCl, 4 mM $MgCl_2$, 0.1 mM $CaCl_2$, 10 mM DTT, and 50 mM TES (pH 7.1). V_{max} obtained from Lineweaver-Burk plots of velocity vs. actin concentration was 13 s^{-1} at 24°C (an average of three experiments).

Unless otherwise stated, actin–S1 complexes were prepared as follows. Free ATP and ADP in the purified G-actin solution were removed by elution through a Sephadex G-25 column (Pharmacia Fine Chemicals, Piscataway, NJ) equilibrated with 2 mM TES (pH 7.1), and the actin was immediately polymerized by mixing with an equal volume of a solution containing 40 mM KCl, 8 mM $MgCl_2$, 0.1 M TES (pH 7.1). The F-actin and the S1 solutions were mixed into 2 ml of rigor solution to final concentrations of 26 and 30 μM. The rigor solution was composed of 20 mM KCl, 4 mM $MgCl_2$, 0.1 mM $CaCl_2$, 10 mM DTT, and 50 mM TES (pH 7.1). The actin–S1 complex was recovered by centrifugation at 45,000 *g* for 30 min in a TL-100 centrifuge (TL-100; Beckman Instruments, Fullerton, CA). The pellet was resuspended in the standard solution (rigor solution containing 5 mM caged ATP) at a concentration of 100 μM each of actin and S1. Aliquots (2–3 μl) of the sample were placed on the surface of a small block (2 mm × 2 mm × 1 mm) of boiled egg white. The drop was drawn off with a filter paper leaving a thin layer of the sample <0.3-mm thick and rapidly frozen. In some samples, the concentration of KCl in the standard solution was changed from 20 mM to 0 or 120 mM. The ionic strength of the standard and modified solutions (0 and 120 mM KCl) was 60, 40, and 160 mM, respectively. Furthermore, in some samples, 0.1 mM $CaCl_2$ in the standard solution was replaced with 1 mM EGTA.

Rapid Freezing and Photolysis of Caged ATP

A rapid freezing device, RF-23 (Eiko Engineering, Ibaraki, Japan), was modified to install the illumination system for the photolysis of caged ATP (see Fig. 1). A new UV light source for photolysis was developed in collaboration with Dr. K. Horiuti (Horiuti et al., 1992): A xenon tube (35S; Chadwick-Helmuth, El Monte, CA) was flashed with a discharge of 200J (2,000 μF, 450 V) with a half-time of ~0.3 ms. Light was collected by an elliptic reflector and a quartz lens into one end of a flexible liquid light guide (φ5 mm, *l* 1 m, NA 0.47; Ultrafine Technology, Bren Hord Middlesex, England). To use only 300–370 nm UV light, a band-pass filter of 270–370 nm (U340; Hoya, Tokyo, Japan) and a cut-off filter of 300 nm (UV30; Hoya) were placed between the lens and the light guide. At the other end of the light guide, light was reflected to illuminate the specimen by means of a reflector (a quartz plano-convex lens [φ10 mm, *f* 15 mm] of which, the flat back surface was coated with aluminum). The reflector was mechanically removed just before the sample collided against the copper block. The specimen on the egg-white cushion was placed on a holder placed at the tip of the plunger, rapidly frozen by being touched to a copper block cooled to 4°K by liquid helium, and stored in liquid nitrogen until use. For freezing the sample, the plunger was set on the freezing device and released to fall freely by tripping a solenoid. The position of the plunger during the fall was detected by a photointerrupter, which regulated the timing of the flash through an electric stimulator. The moment of freezing was detected by measuring the changes in the electric capacitance of the specimen (Heuser et al., 1979).

Deep-Etch, Rotary-Shadow Replica EM

A rapidly frozen sample was mounted in an ultramicrotome (ULTRACUT; Reichert-Jung Optische Werke AG, Wien, Austria) equipped with a low temperature sectioning system (FC4E), and then fractured with a glass knife at −150°C. To avoid being frosted on the fractured surface, the sample was quickly placed on a holder, covered with a cooled cap, then transferred to freeze-etch equipment (BAF 400D; Balzers Union Aktiengesellschaft, Liechtenstein, Germany) in a nitrogen atmosphere. When a vacuum of 2 × 10^{-6} torr was achieved at −150°C, the sample holder was warmed up to −100°C and immediately the cooled cap covering the sample was removed. The sample was etched for 7 min followed by rotary shadowing with platinum–carbon and carbon angles of 25° and 65°, respectively. In our etching procedure, the exact temperature of the sample itself, when the covering cap is removed, is unknown (within −150 ~ −100°C), since at that timing the temperature of the sample is not expected to be equal to that of the sample holder (−100°C). To avoid the collapse of samples and the deposition of salts, the minimum etching depth must be maintained. Therefore, according to the criteria that ice should be seen in the background, the optimal etching time was determined to be 7 min in our system to make the etching as shallow as possible. Under this etching time, almost all filaments observed reproducibly looked free from collapse.

The sample was removed from the freeze-etch device and immersed in methanol at −20°C overnight. The sample was dissolved in household bleach, and replicas floating off the sample were washed three times with distilled water and picked up on formvar-filmed grids. Stereo pair electron micrographs were taken at a magnification of ×25,000 on a JEM-1200EX electron microscope (JEOL, Tokyo, Japan) operated at 100 kV by tilting the specimen stage at ±10°. Electron microscopic negatives (Fuji Electron Microscopic film FG; Fuji Photo Film, Tokyo, Japan) were reversed onto Ko-

dak fine grain positive film 7302 (Eastman Kodak, Rochester, NY), and then printed as negative images.

In this study, we obtained images from at least four different frozen samples at several time after photolysis (15, 20, 25, 30, 35, 40, 65, 80, 100, 200 ms under each condition), and ~2,000 micrographs were taken in total.

Measurement and Analysis of the Angle of S1 to Actin Filaments

Stereo pair electron micrographs were enlarged to a final magnification of ×250,000. To determine the distribution of S1–actin angles as accurately as possible without bias, a blind test was performed by four different persons, two of whom had no information of the purpose and design of this study. Each person measured angles of 150–300 S1 molecules under each condition of rigor, 25, 35, and 100 ms after the photolysis of caged ATP. Only S1 molecules attached at the side of actin filaments were selected to measure the angle of S1 to actin filaments.

Although it would be a little bit arbitrary, we assumed that the majority of the S1 molecules are pointed toward the pointed end of the actin filament for both the rigor and ATP samples. As compared to the rigor sample, in the presence of ATP the establishment of the actin polarity was not easy when only a few S1 molecules were identified on a single actin filament, probably because in the ATP sample S1 molecules have a tendency to take various angles. Therefore, actin filaments associated with more than 5 S1 molecules were selected, and their polarity was determined by the inclination of the majority of S1 molecules. Measured angles for S1 pointing toward the pointed end were assigned as 0–90°, and those for S1 pointed away from the pointed end as 90–180°. The statistical test was performed within each set of angle distributions (rigor, 25, 35, and 100 ms after photolysis) obtained by each observer according to the Kolmogorov-Smirnov test.

Distribution of the Distance of the Nearest-neighbor S1 on Actin Filaments in Electron Micrographs and in Computer Simulation

Stereo pair electron micrographs were enlarged to a final magnification of ×200,000. The position of S1 attached to actin was input to a micro computer through a digitizer, and the distribution of the distance of the nearest neighbor S1 was calculated. The magnification of electron micrographs was calibrated by 5.5-nm pitch of actin filaments and 35.5-nm half-pitch of actin–S1 complex.

Computer simulation of the binding of ~1,000 S1 molecules to actin filaments consisting of ~6,000 actin monomers was performed. To evaluate the effect of the cooperative binding of S1 on the distribution of the distance of the nearest neighbor S1 on actin filaments, we assumed that the binding of one S1 molecule to one actin monomer facilitated the binding of another S1 molecule to the adjacent actin monomer by a factor of 5 or 2, and suppressed it by a factor of 1/2 or 1/5.

Computer Simulation of the Behavior of S1 after Photolysis of Caged ATP

The rate constant of the photolysis of caged ATP is 118 s^{-1} at 20°C, and Q_{10} is 2.3 (McCray et al., 1980; Goldman et al., 1984). Taking it into consideration that the surface temperature of the sample is expected to be 15°C (dew point), the rate constant of ATP release from caged ATP (see k_0 in Fig. 10) was calculated to be 80 s^{-1} in our experimental condition. The rapid equilibrium of S1 dissociation from and association with actin at association constants of 1×10^4 M^{-1} (K_2 in Fig. 10) and 3×10^3 M^{-1} (K_4) were assumed (Chalovich and Eisenberg, 1981). Other rate constants were set as follows: $k_3 = 30$ s^{-1}, $k_{-3} = 20$ s^{-1}, $k_5 = 12$ s^{-1}, $k_{-5} = 28$ s^{-1}, $k_6 = 85$ s^{-1} (Rosenfeld and Taylor, 1984), and $k_7 = 400$ s^{-1} (Siemankowski et al., 1985). The differential equations of the kinetic scheme (see Fig. 10 *A*) were solved by the Euler method. To fit the calculated time course of the total number of actin-bound S1 to our electron microscopic observation, various values of second-order rate constant for dissociation of S1 with respect to ATP (k_1 in Fig. 10) were tested.

Results

Development of a New Rapid Freezing System Coupled with the Caged Compound Technique

To develop a new freezing system for EM which permits the photolysis of caged ATP in the actin-S1 complex just before rapid freezing (Fig. 1), the following technical problems had to be solved. The first was how to introduce the intense UV light to the specimen on the tip of the plunger just before freezing. A new light box was developed using a xenon tube (Horiuti et al., 1992). The emitted light was transmitted to the tip of the plunger through a flexible liquid light guide and reflected to illuminate the sample by a reflector. Just before

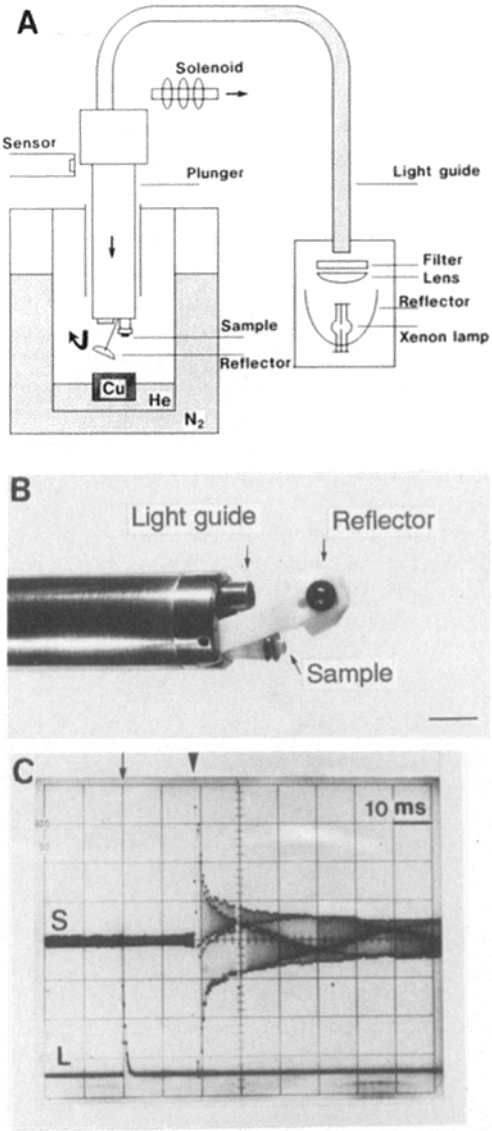

Figure 1. (*A*) Diagram of the rapid-freezing apparatus which permits the photolysis of caged ATP. The ultraviolet light pulse from a xenon tube was introduced to a specimen on the tip of the plunger through a flexible liquid light guide and a reflector. The reflector was removed just before the specimens were hurled against the copper block (*Cu*) cooled to 4°K by liquid helium (*He*). The position of the plunger was detected by a sensor and the timing of the flash was controlled by an electric stimulator. (*B*) Tip of the plunger. (*C*) Oscilloscope traces showing the timing of the flash and freezing. The change in specimen capacity was measured by applying a 100 kHz oscillating signal to the specimen (*S*), which showed the moment of freezing (*arrowhead*) and the rate of freezing. The intensity of the UV light was monitored as an out put of a photodiode (*L*) to determine the timing of the flash (*arrow*). In this example, the sample was frozen at 18 ms after the UV flash. Bar, 1 cm.

freezing, this reflector was mechanically removed to avoid direct collision against the copper block. Therefore, in our system, the timing of removing the reflector determined the shortest possible duration from photolysis to freezing; 13 ms. By placing a film at the position of the specimen at the tip of the plunger, we confirmed that the sample was evenly and diffusely illuminated. In this illumination system, a luciferin–luciferase assay revealed that a single flash splits 15.5 ± 2.6% (±SD, $n = 6$) of caged ATP in the absence of proteins. We further confirmed by Pi measurements that the efficiency of ATP release was not affected by acto-S1 complexes in the sample. Since the standard solution used in this study contained 5 mM caged ATP, the concentration of photoreleased ATP in the sample was expected to be 750 μM. Considering that the sample is a very thin layer <0.3-mm thick and that only the layer within 10 μm from the surface is observed, the absorption of UV light by proteins and caged ATP can be neglected.

The second problem was sample denaturation by the intense UV light. This type of damage was minimized by placing band-pass and cut-off filters between the lens and the light guide to use only 300–370 nm UV light (see Materials and Methods; Horiuti et al., 1992). We especially paid attention to filter out the 280–300 nm light to prevent absorption of energy by proteins. The liquid light guide itself was also expected to function as a heat absorption filter. As shown later in this study, most of the myosin heads attached to actin filaments in a state of rigor were quickly released by UV illumination under low protein concentration (see Fig. 5) or high ionic strength conditions (data not shown). This result excluded the possibility that some of the S1 molecules became cross-linked to the actin filaments by irradiation of UV light. Furthermore, the S1 molecules reassociated with filaments after the consumption of photoreleased ATP (data not shown). These observations led us to conclude that in our illumination system, the UV damage to proteins can be minimized.

The third problem was how to regulate and record the timing of flashing and/or freezing. To gain reproducibility in the duration from the moment of flashing to that of freezing, the plunger was set on the freezing apparatus and released to fall freely towards the copper block by tripping a solenoid. The

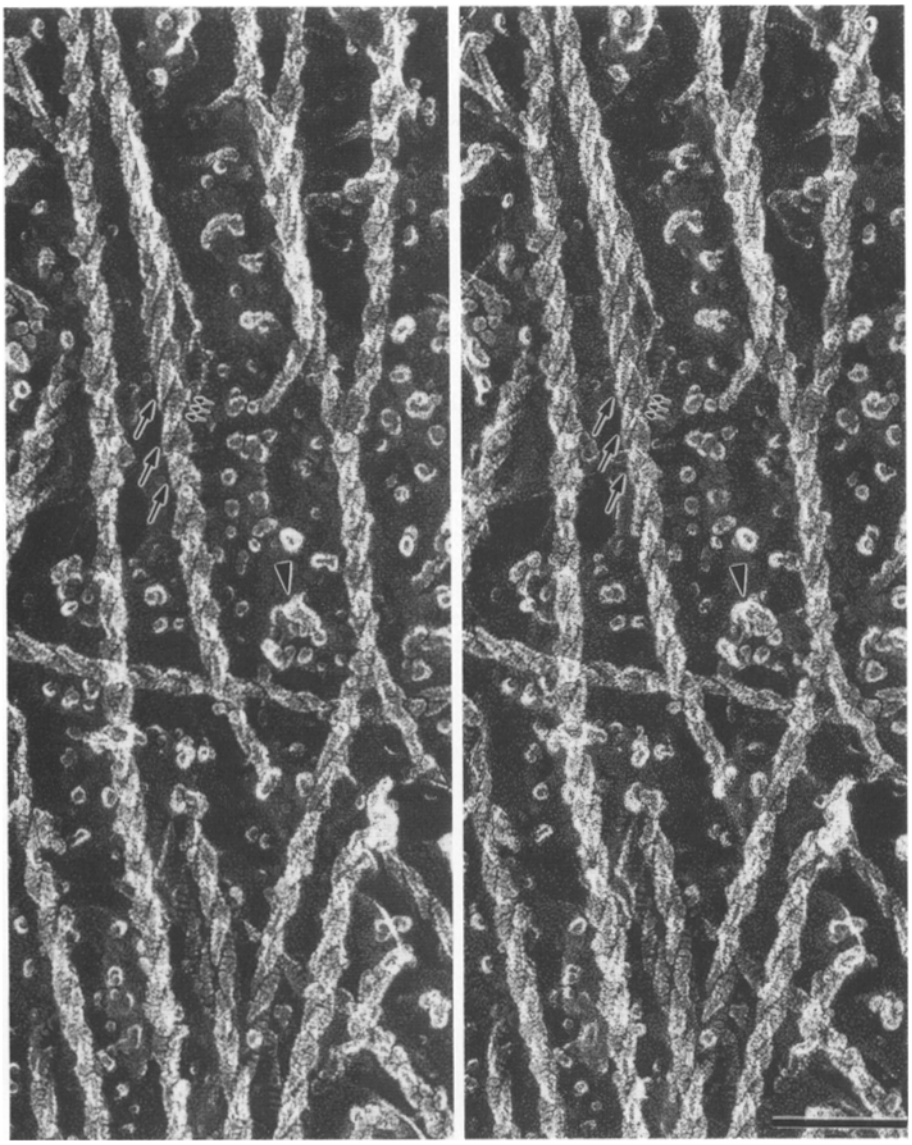

Figure 2. Stereo pair micrographs of a freeze-etch replica of actin filaments fully decorated with S1 in the presence of caged ATP. Acto-S1 complexes (100 μM) in the standard solution (20 mM KCl, 4 mM $MgCl_2$, 5 mM caged ATP, 0.1 mM $CaCl_2$, 10 mM DTT, 50 mM TES, pH 7.1; ionic strength = 60 mM) were rapidly frozen. This complex is characterized by ropelike right-handed double helices with half pitch of 35 nm (*large arrows*). Note the 5.5-nm striation on the surface of each rope which comes from closely packed S1 molecules (*small arrows*). Some complexes are seen to protrude from the ice (*arrowheads*). Bar, 100 nm.

position of the plunger was detected by a photointerrupter, and the timing of the flash was controlled by an electric stimulator. The moment of freezing and the rate were measured by detecting the change of the electric capacitance of the specimen mainly according to the method developed by Heuser et al. (1979). Fig. 1 *C* shows an example of measurements at the moments of flashing and freezing on an oscilloscope. In this example, the specimen touched the copper block at 18 ms after the UV flash.

Structure of Actin Filaments and Actin–S1 Complex in the Presence of Caged ATP

We checked whether caged ATP affect the structure of the actin filaments and the actin–S1 complex. A suspension of actin filaments (200 μM) was rapidly frozen in the presence of caged ATP (in the standard solution) and a deep-etch replica image was obtained (data not shown). Actin filaments had striations of 5.5 nm on their surface which corresponded to a genetic helix (Hanson and Lowy, 1963; Heuser and Kirschner, 1980; Heuser and Cooke, 1983). There were only a few particles on actin filaments, which may have been the deposition of G-actin or salts. Hardly any structural differences were discerned between actin filaments in the presence and absence of caged ATP (data not shown).

Fig. 2 shows the deep-etch replica image of actin filaments fully decorated with S1 in the presence of caged ATP. To avoid the collapse of samples and the deposition of salts, the minimum etching depth was rigorously maintained, so that ice was seen in the background. These filaments were characterized by a ropelike double helix appearance (35 nm half pitch) and by striations of ~5.5 nm on their surface derived from S1 molecules closely packed along them (Heuser and Kirschner, 1980). Since the actin–S1 complexes were randomly oriented in the sample, some of them were seen to protrude from the ice. These images again appeared to be identical to those in the absence of caged ATP. These data clearly revealed that caged ATP (5 mM) showed no structural effects either upon actin filaments or upon actin–S1 complexes.

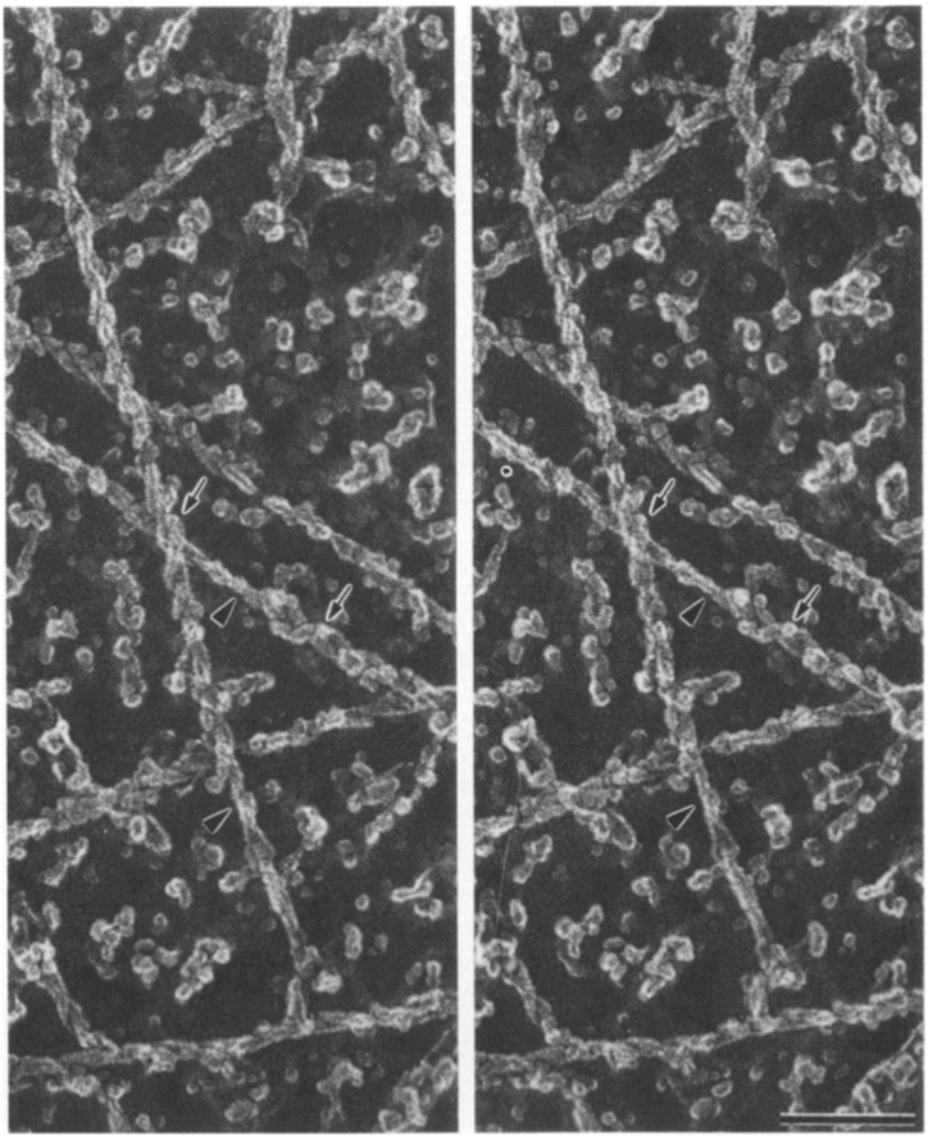

Figure 3. Stereo pair micrographs of a freeze-etch replica of an actin–S1 complex (100 μM) frozen at 15 ms after the photolysis of caged ATP. The ropelike helical appearance is still prominent in most of the filaments, but are irregular and thinner. Note that some areas are densely decorated in a helical manner (*arrows*), while others are sparsely decorated with a loose helical appearance (*arrowheads*). Bar, 100 nm.

Behavior of S1 on Actin Filaments after Photolysis of Caged ATP

To analyze the transition from the rigor state to the steady state in the presence of ATP, the ropelike actin–S1 complex containing 5 mM caged ATP was illuminated with a UV flash, and the induced structural changes were pursued by rapid-freeze EM. A single UV flash split 750 μM ATP from 5 mM caged ATP. Fig. 3 shows a deep-etch replica image of the actin–S1 complex frozen at 15 ms after the photolysis of caged ATP. The ropelike helical appearance was still prominent in most parts of the filaments, but became irregular and thinner, indicating that some S1 has already gone from filaments. Hardly any bare actin filaments were observed. Close inspection revealed that along single filaments, the density of attached S1 was not constant. Some parts were densely decorated in a helical manner, while others were sparsely decorated with a loose helical appearance. These images were reproducibly obtained at 15 ms after photolysis, indicating that the samples were uniformly illuminated and that the duration between flashing and freezing was reproducible.

At 25 ms after the photolysis of caged ATP, the ropelike appearance vanished and each S1 became distinguishable (Fig. 4). The filaments were mostly covered with S1, but the bare surface of actin filaments with 5.5 nm striations was occasionally observed through small openings between S1 molecules. The number of S1 molecules bound to actin filaments decreased gradually up to 35 ms after the photolysis, and at 35 ms, the bare surface became dominant although many S1 molecules still remained on the filaments (see Fig. 7, *D–F*). The S1 density on actin filaments at 35 ms was ~20% of that of fully decorated filaments. We further pursued the structural changes of actin–S1 complex (40, 65, 80, 100, and 200 ms after the photolysis of caged ATP), but the images obtained from these samples were indistinguishable from those at 35 ms. This indicated that, under the conditions used in this study, the dissociation–association equilibrium between S1 and actin filaments reached the steady state in the presence of ATP within 35 ms after the photolysis of caged ATP. We also examined the S1 behavior at low Ca concentrations (in the standard solution containing 1 mM EGTA instead of

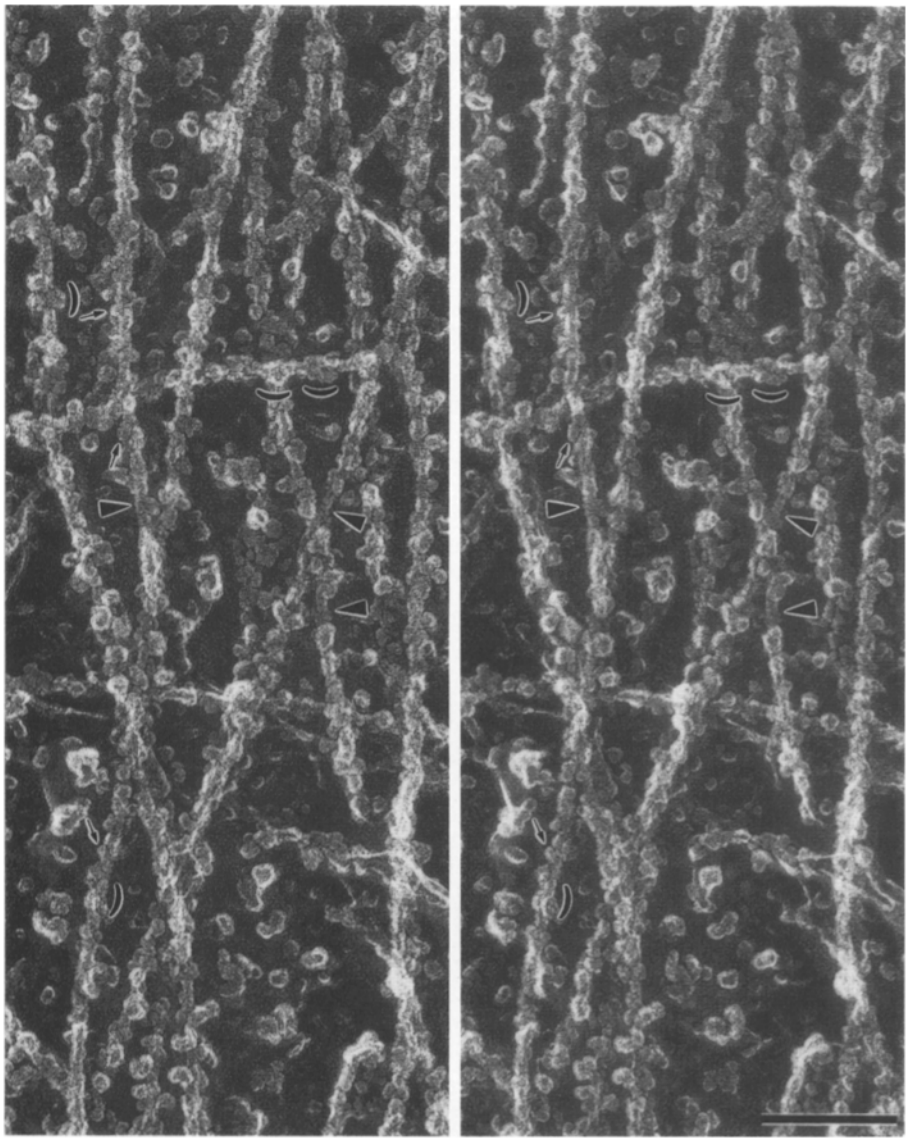

Figure 4. Stereo pair micrographs of a freeze-etch replica of an actin–S1 complex (100 μM) frozen at 25 ms after the photolysis of caged ATP. The ropelike appearance is undetectable and each individual S1 molecule can be identified on actin filaments (*small arrows*). The actin filaments are mostly covered with S1 molecules, but the bare surface of actin filaments with 5.5-nm striations is occasionally observed through the small openings between S1 molecules (*arrowheads*). The S1 molecules appear to be clustered on filaments (*parentheses*). Bar, 100 nm.

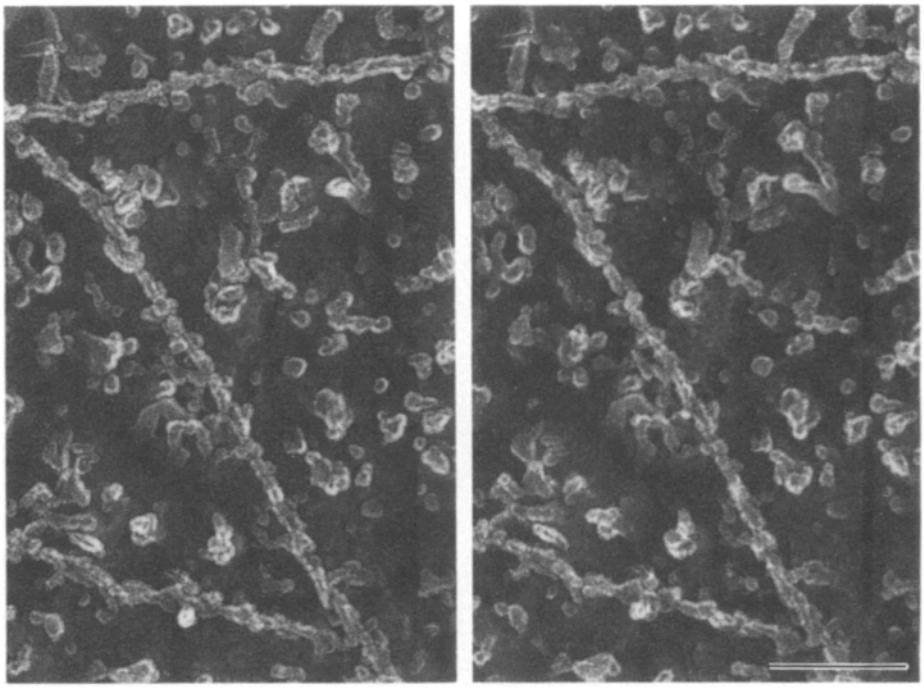

Figure 5. Stereo pair micrographs of a freeze-etch replica of an actin–S1 complex (low protein concentration; 40 μM) frozen at 15 ms after the photolysis of caged ATP. When compared with Fig. 3, the number of S1 molecules on actin filaments had remarkably decreased. Bar, 100 nm.

0.1 mM $CaCl_2$), and obtained similar results (data not shown).

Effects of Protein Concentration and Ionic Strength on the Behavior of S1 on Actin Filaments after the Photolysis of Caged ATP

To confirm that S1 molecules were in rapid association to and dissociation from actin in the presence of ATP, the behavior of S1 on actin filaments was examined at a lower protein concentration. The concentration of both actin and S1 was reduced to 40 μM (100 μM in the above experiments). Under these conditions, at 15 ms after the photolysis, the attached-S1 had already remarkably decreased in number (Fig. 5) and at 25 ms, only a small number of S1 molecules were observed on the bare actin filaments (data not shown). A comparison of Fig. 5 with Fig. 3 indicated that the association/dissociation between S1 and actin filaments had occurred even at 15 ms, and that our electron microscopic images did not represent the simple dissociation process of strongly bound S1 but the more complicated association/dissociation process.

Next, we examined the effect of ionic strength on the behavior of S1 on actin filaments. Acto-S1 (100 μM) in the higher or lower salt solution (160 mM and 40 mM of ionic strength, respectively) was rapidly frozen after flashing as in the above experiments. At 100 ms after photolysis, under conditions of higher ionic strength (160 mM), only ~5% of total S1 molecules were detected on actin filaments, whereas at lower ionic strength (40 mM), ~40% of total S1 molecules on filaments (data not shown). As shown above, at the ionic strength of 60 mM, ~20% of total S1 molecules were observed on actin filaments. These results excluded the possibility that the free S1 molecules floating around actin filaments in solution might be deposited upon them during freeze etching. Considering that the affinity of S1 molecules to actin filaments in the presence of ATP increases with a decrease in ionic strength (Greene et al., 1983; Katoh and Morita, 1984), almost all S1 molecules observed on actin filaments in our replica images were rapidly frozen during direct interaction at the time of freezing.

Conformation of Actin–S1 Complex in the Absence or Presence of ATP

To visualize individual S1 molecules on actin filaments in the absence of ATP, S1 was mixed with actin filaments at a molar ratio of 1:5 (20 μM S1 and 100 μM actin) in the standard solution, and then frozen without the photolysis of caged ATP (Fig. 6). Since S1 reportedly bundles actin filaments at this molar ratio (Ando and Scales, 1985), samples were frozen immediately after mixing. In the deep-etch replica images of this sample, individual S1 molecules appeared spheroidal ~16 and 8 nm in major and minor axes, respectively.

Next, we compared the conformation of S1 molecules in the absence and presence of ATP (Figs. 6 and 7). Within the resolution of the deep-etch replica technique, no significant conformational difference was discernible. Close inspection however, revealed that the angle of S1 molecules to actin filaments appeared to be affected by ATP. To determine the S1-actin angles as accurately as possible without bias, four observers (T. Funatsu, E. Kono, T. Wazawa, and Y. Yasuda) measured the angles without being given any information about the images (blind teat) (see Figs. 6 *F* and 7 *G*). To examine the distribution of S1–actin angles under each condition (rigor, 25, 35, and 100 ms after photolysis), we selected rather long actin filaments associated with more than 5 S1 molecules and determined the polarity of each filament as described in detail in Materials and Methods. As shown in Figs. 6 and 7, the establishment of the filament polarity was easier in the rigor sample than in the ATP sample, because ATP appeared to decrease the tilt of S1 from the perpendicular to the filaments. Even in the rigor sample, some S1 molecules were observed to tilt to point in the direction opposite to the majority of S1 (Fig. 6). Each angle was assigned from

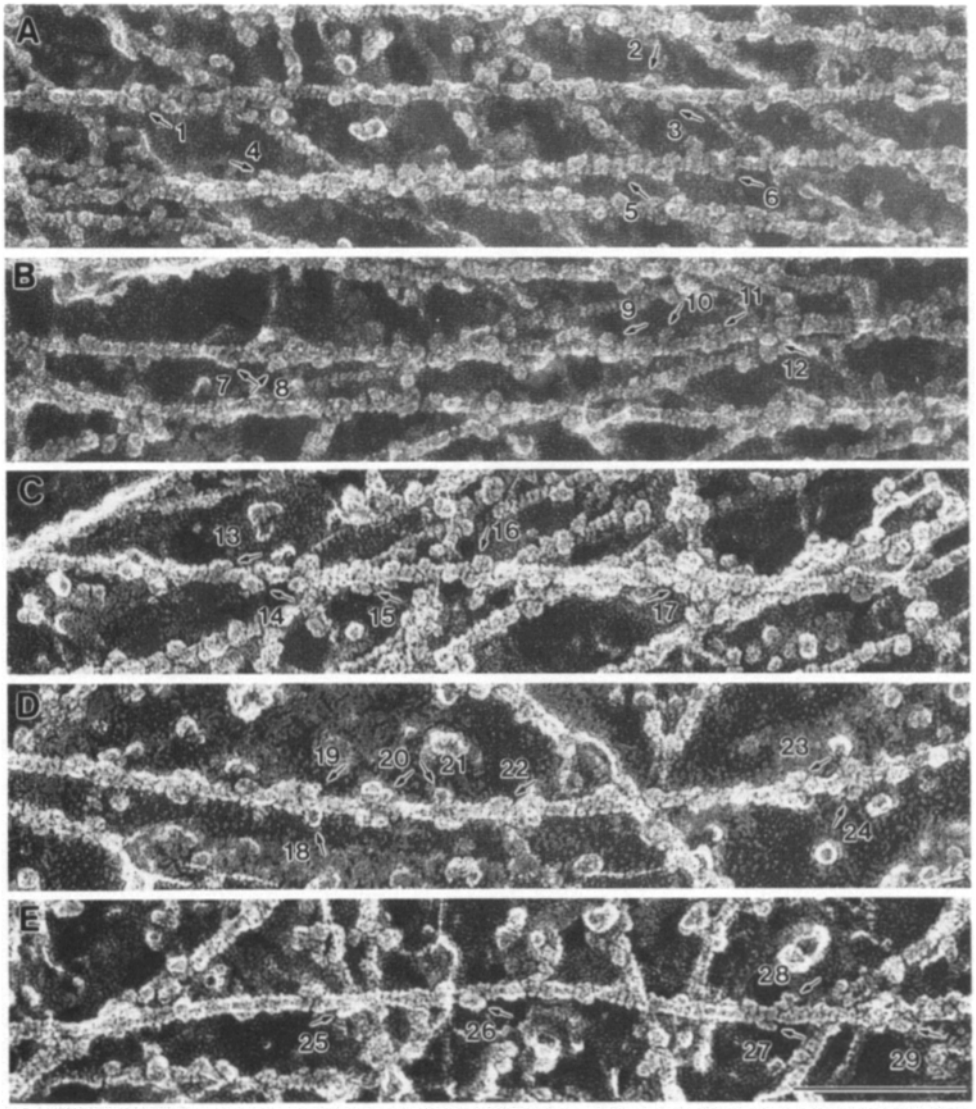

F

No.	1	2	3	4	5	6	7	8	9	10	11	12	13	14	15	16	17	18	19	20	21	22	23	24	25	26	27	28	29
T.F.	2	0	0	1	0	0	2	0	0	0	0	2	0	0	0	3	0	1	0	0	0	2	0	0	0	2	0	0	0
E.K.	0	0	0	0	0	0	0	0	0	0	0	3	0	0	0	0	0	0	0	3	0	2	0	0	0	0	1	0	0
T.W.	2	3	0	0	0	0	2	2	0	0	0	0	2	2	0	0	0	0	3	3	0	0	0	0	0	0	1	0	
Y.Y.	0	2	0	0	0	0	0	0	0	2	0	0	0	2	0	3	0	0	0	3	0	2	0	0	2	0	0	1	0

Figure 6. Individual S1 molecules on actin filaments in the absence of ATP. (*A–E*) Actin and S1 were mixed at a molar ratio of 5:1 (100 μM actin and 20 μM S1) just before rapid freezing in a rigor solution (20 mM KCl, 4 mM $MgCl_2$, 0.1 mM $CaCl_2$, 10 mM DTT, 50 mM TES, pH 7.1) containing 5 mM caged ATP. Arrows indicate the attachment angle of S1 molecules scored by at least one of four observers. (*F*) Selection of S1 molecules to be scored. Numbers correspond to S1 molecules indicated by arrows in *A–E*. Observers: T. Funatsu (T. F.), E. Kono (E. K.), T. Wazawa (T. W.), Y. Yasuda (Y. Y.). *0*, *1*, *2*, *3* represent the following situations. The structure on filaments was identified as an S1 molecule and scored (*0*), was not identified as S1 (*1*), was identified as S1 but not scored since its orientation was not good for measurement (*2*), and was identified as S1 but not scored since it was deformed by association with adjacent S1 (*3*). Bar, 100 nm.

0° to 180°: the angles of S1 pointing toward and away from the pointed end were defined to fall in 0–90° and 90–180°, respectively.

The distribution of angles was then compared between the samples frozen in the absence of ATP and at 35 ms after the photolysis of caged ATP (Fig. 8). As shown in Figs. 6*F* and 7*G*, although observers had been asked to select S1 molecules attaching at the side of filaments, observers differed in selection of S1 molecules. In spite of the difference, four observers obtained similar results on the distribution of S1-actin angles: The observer-dependent difference of the peak was within 10°. Therefore, in Fig. 8, the distribution averaged from the data by four observers were shown. As shown in Fig. 8, *A* and *B*, both in the rigor and 35-ms samples, two peaks were detected (around 30° and 160°). As shown in Fig. 8 *C*, comparison of these distribution revealed that ATP made the 30° peak small whereas the 160° peak was less sensitive to ATP, and that in the 35-ms sample, the S1 showing 60–120° increased in number. As a result, the S1 molecules in the 35-ms samples showed a broader angle distribution as compared to those in the rigor sample. At present, it is not clear what the ATP-insensitive 160° peak is. Considering that S1 reportedly bundles actin filaments under the condition used in this study (Ando and Scales, 1985), one possible explanation for the 160° peak is that S1 has an ATP-independent binding mode to actin filaments with its tail region and that this binding mode gives the ATP-insensitive 160° peak.

The difference in the angle distribution between the rigor and 35-ms samples was statistically evaluated for the data obtained by each observer. According to the Kolmogorov-Smirnov test, the difference in the angle distribution between the rigor and 35-ms samples was statistically significant at

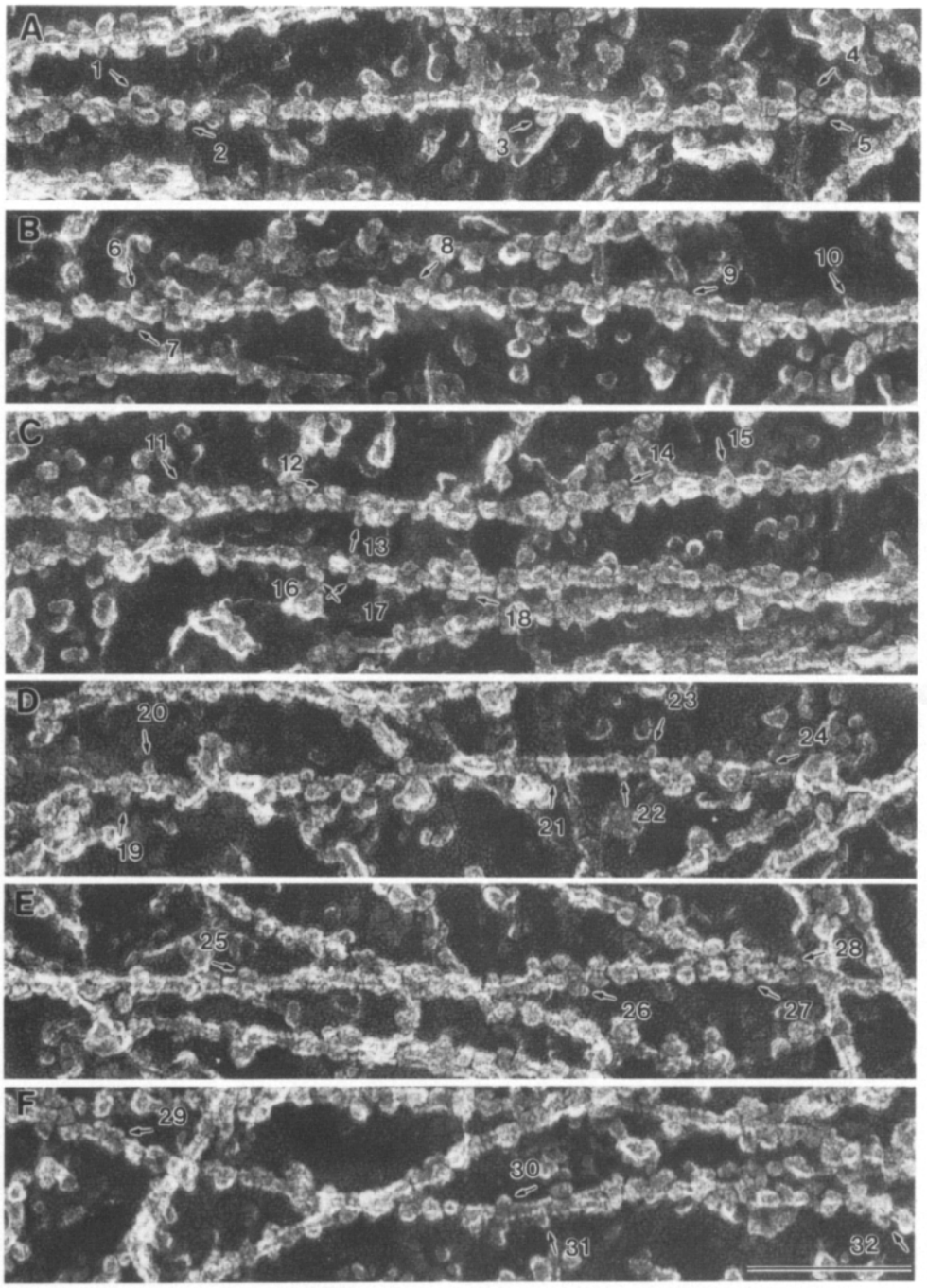

G

No.	1	2	3	4	5	6	7	8	9	10	11	12	13	14	15	16	17	18	19	20	21	22	23	24	25	26	27	28	29	30	31	32
T.F.	1	0	3	0	0	0	0	0	0	0	0	0	0	0	2	0	0	2	0	0	2	2	0	0	0	0	2	0	0	2	0	0
E.K.	0	0	0	0	0	0	0	2	0	2	0	0	3	2	0	0	2	2	0	0	0	0	0	0	0	0	0	0	0	0	0	0
T.W.	0	0	3	0	0	0	3	0	2	2	0	0	3	0	2	0	0	0	3	3	0	0	0	2	0	0	0	2	0	0	0	2
Y.Y.	0	0	0	0	2	0	3	3	0	3	3	0	3	0	2	0	0	0	0	0	2	2	0	0	0	0	0	0	0	2	0	0

Figure 7. Individual S1 molecules on actin filaments in the presence of ATP. At 25 (*A*, *B*, and *C*) and 35 ms (*D*, *E*, and *F*) after the photolysis of caged ATP. Arrows indicate the attachment angle of S1 molecules scored by at least one of four observers. (*G*) Selection of S1 molecules to be scored. See details in the legend of Fig. 6 *F*. Bar, 100 nm.

accuracy of ≥95–99% (for T. Funatsu, E. Kono, T. Wazawa), and ≥90-95% (for Y. Yasuda). Also in the 25- and 100-ms samples, the angle distribution was analyzed (data not shown). The distribution of 25-ms sample appeared to be an intermediate between the rigor and 35-ms samples, while that of the 100-ms sample was very similar to that of the 35-ms sample.

Cooperativity in the Binding of S1 to Actin Filaments in the Absence or Presence of ATP

Both in the absence or presence of ATP (35 and 100 ms after photolysis), the distribution of the distance of nearest-neighbor S1 molecules on actin filaments was examined (Fig. 9). Partially decorated actin filaments as shown in Fig. 6

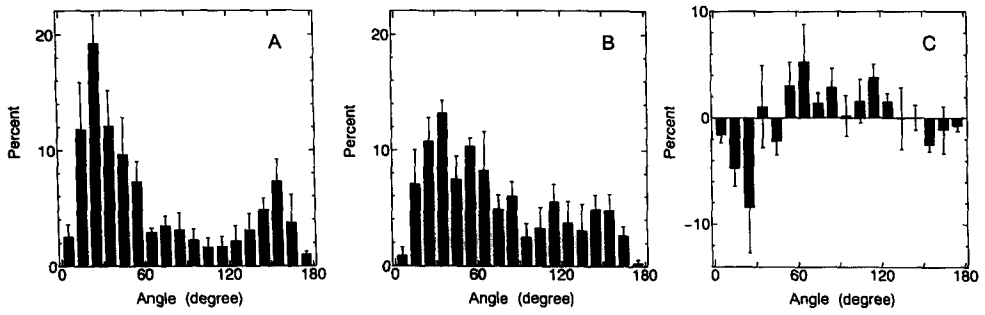

Figure 8. Distribution of the binding angle of S1 to actin filaments under conditions of rigor (*A*) and 35 ms after photolysis (*B*). (*C*) The ATP-dependent change of S1-actin angles. This was obtained by subtracting *A* from *B*. The method how to select S1 molecules and determine the filament polarity was described in detail in Materials and Methods. The angle of S1 pointing toward and away from the pointed end of filaments was defined to fall in 0–90° and 90–180°, respectively. Angle was scored by four observers in a blind test. Each observer scored 150–300 S1 for each condition. Average ±SD of four observers were represented by bars.

were used as a rigor sample. To determine the effect of the cooperativity on the distribution of the distance of nearest-neighbor S1 on actin filaments, a computer simulation of the S1 binding was performed (see details in Materials and Methods).

Both in the absence and presence of ATP, when the binding of one S1 molecule to one actin monomer was assumed to suppress the binding of another S1 molecule to the adjacent actin monomer by the factor of 1/2, the best fit was obtained in the distribution of the distance of nearest-neighbor S1 between our experiments and the computer simulation. Therefore, S1 molecules did not show any positive cooperativity in their binding to actin filaments in the absence or presence of ATP under our experimental conditions.

Discussion

We have developed a new freezing system for EM which permits the photolysis of caged ATP in the actin–S1 complex immediately before rapid freezing. Using this system combined with the deep-etch replica method, we captured the behavior of S1 on actin filaments at each step of the transition from the rigor state to the steady state in the presence of ATP. While developing this freezing system, we checked many artifacts which could be introduced and tried to avoid them (see Results). Finally, we conclude that the dynamic structural changes of actin–S1 complex observed in this study were in fact triggered only by an abrupt increase of the concentration of ATP, and that among all S1 molecules, only S1 molecules attached to actin filament were selectively observed as clear particles on actin filaments.

It has been assumed that caged ATP is physiologically inert. Detailed analyses on the rotational motion of spin-labeled S1 (Berger et al., 1989) and the stiffness of muscle fibers (Goldman et al., 1984) revealed that S1 assumed a rigor conformation in the presence of caged ATP. In fact, as shown in Figs. 2 and 6, S1 takes this conformation even in the presence of caged ATP.

The S1 behavior after photolysis of caged ATP was characterized as follows under our conditions: (*a*) The actin filament-associated S1 decreased in number gradually up to 35 ms after the photorelease of ATP; and (*b*) At 35–200 ms after the photolysis, the number of attached S1 remained constant. To interpret these results, a computer simulation of the behavior of S1 after photolysis of caged ATP was performed using parameters obtained from published actomyosin biochemistry (Fig. 10, *A* and *B*). Taking it into consideration that the photolysis dark reactions of caged ATP delay the dissociation of S1 from actin filaments (see details in Materials and Methods), the second-order rate constant of 3×10^5 $M^{-1}s^{-1}$ for dissociation of S1 with respect to ATP gave the best fit to our electron microscopic observations that are summarized above as *a* and *b*. This value is comparable to $1\text{–}10 \times 10^5$ $M^{-1}s^{-1}$ determined by applying caged ATP to muscle fibers (Goldman et al., 1984; Horiuti et al., 1992) or acto-S1 complexes (McCray et al., 1980), and somewhat smaller than $10\text{–}40 \times 10^5$ $M^{-1}s^{-1}$ obtained by the stopped-flow method with acto-S1 complexes (White and Taylor,

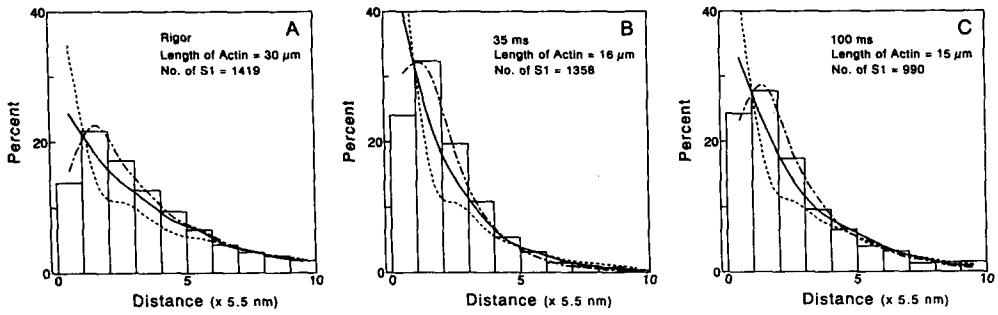

Figure 9. Distribution of the distance between the nearest-neighbor S1 molecules on actin filaments. (*A*) rigor; (*B*) 35 ms; and (*C*) 100 ms after the photolysis of caged ATP. Computer simulation results are shown by lines (see details in Materials and Methods). (——) Independent binding of S1 along actin filaments; (– – –) positive cooperativity in the binding of S1 by a factor of 2; (·····) negative cooperativity in the binding of S1 by a factor of 1/2.

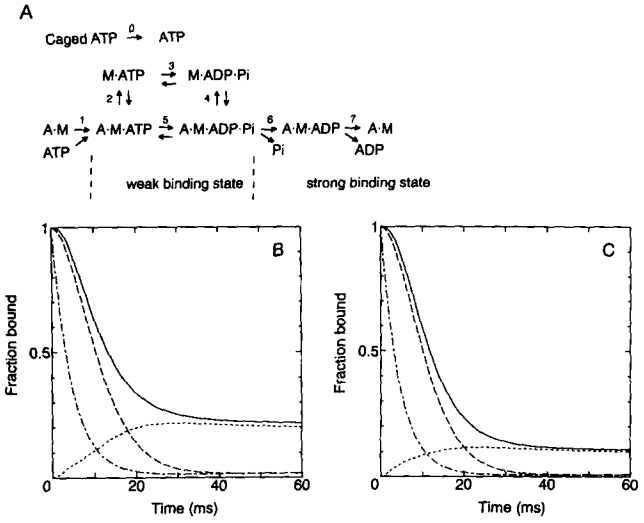

Figure 10. Computer simulation of the behavior of S1 after photolysis of caged ATP using published actomyosin biochemistry. (*A*) A kinetic scheme of the photolysis of caged ATP and the elementary steps of actomyosin ATPase. *A* and *M* represent actin and myosin subfragment 1, respectively. Strongly and weakly bound S1 correspond to A·M·ADP/A·M and A·M·ATP/A·M·ADP·Pi, respectively. (*B* and *C*) Simulation of the behavior of S1 after 100 μM (*B*) and 40 μM (*C*) acto-S1 complexes containing caged ATP is flashed with UV light under the condition used in this study. The rate constants used were $k_0 = 80\ s^{-1}$; $k_3 = 30\ s^{-1}$; $k_3 = 20\ s^{-1}$; $k_5 = 12\ s^{-1}$; $k_{-5} = 28\ s^{-1}$; $k_6 = 85\ s^{-1}$; $k_7 = 400\ s^{-1}$. Association constants of $K_2 = 1 \times 10^4\ M^{-1}$ and $K_4 = 3 \times 10^3\ M^{-1}$ were assumed (see details in Materials and Methods). To obtain the best fit to our electron microscopic observations, the second-order rate constant with respect to ATP for dissociation of S1 was assumed to be $3 \times 10^5\ M^{-1}s^{-1}$. (– – –) Fraction of strongly bound S1; (· · · · ·) fraction of weakly bound S1; (——) fracton of total bound S1; (-·-·-) fraction of strongly bound S1 calculated assuming that UV flash converts caged ATP to ATP without delay.

1976; Goldman et al., 1984). The difference might be ascribed to the binding of higher affinity isomer of caged ATP to S1, which was reported to slow the relaxation of muscle fibers (Dantzig et al., 1991). This computer simulation tells us that our present electron microscopic observations are highly consistent with published actomyosin biochemistry, and that even from 15 to 35 ms after the photolysis we observed not only the dissociation process but also the reassociation process of S1 molecules.

Under our experimental conditions, the interaction between actin filaments and S1 reached a steady state at 35 ms after photolysis, which continued at least up to 200 ms. According to the computer simulation, the actin filament-attached S1 molecules from 35 to 200 ms are mostly actin.S1.ATP or actin.S1.ADP.Pi. This interpretation is favored by the images obtained under conditions of low protein concentration and high ionic strength; both of which shift the equilibrium to the dissociation side, resulting in a remarkable decrease of the number of S1 on actin filaments (see Figs. 3 and 5). Actually, the remarkable decrease of the number of actin filament-attached S1 under the condition of low protein concentration can be simulated by the computer calculation (Fig. 10 *C*). Based on these interpretations, we conclude that by using EM, we captured instantaneous views of weakly bound S1 on actin filaments (actin.S1.ATP and actin.S1.ADP.Pi), which are under rapid equilibrium between association with and dissociation from actin filaments in the presence of ATP.

The time course of the formation of weakly bound S1 observed in this study was highly consistent with that reported from the analyses of muscle contraction using stiffness measurements and caged ATP. The main advantage of EM is being able to obtain simultaneous structural information. Thus, we attempted to analyze whether the weakly and strongly bound S1 differ conformationally. Recently, the ATP-dependent conformational change of S1 was reported to be captured by small angle X-ray scattering (Wakabayashi et al., 1992). Although we had the impression that some S1 molecules appeared to be shorter and fatter in the presence of ATP than in the absence as claimed previously (Craig et al., 1985; Applegate and Flicker, 1987; Katayama, 1989), it was not confirmed mainly due to the limitation of the space resolution of the deep-etch replica method. As far as this method could resolve, the most characteristic aspect of the weakly bound S1 was that its angle distribution is significantly broader than that of rigor S1 (Fig. 8). The broad distribution of the attachment angle of the weakly-bound S1 is consistent with the data obtained from EPR (Berger et al., 1989), X-ray diffraction (Matsuda and Podolsky, 1984), X-ray scattering (Lowry and Poulsen, 1987), and mechanical studies of muscle fibers (Brenner et al., 1982, 1984). The broad distribution of the attachment angle of S1 favors the idea that conformation of S1 does not necessarily correspond to chemical state of S1 during ATPase cycle in one to one fashion.

The other issue is whether there is cooperativity in the binding of S1 molecules to actin filaments in the presence of ATP. It has been reported that S1 binds independently along pure actin filaments both in the presence and in the absence of an ATP analog (Green and Eisenberg, 1980; Trybus and Taylor, 1980). This conclusion was obtained from biochemical studies using Scatchard plots. This method is not applicable in the presence of ATP partly due to the low affinity of S1 for actin filaments and partly to the depletion of ATP during the experimental procedure. Direct visualization of weakly bound S1 using our freezing system may be the only way to evaluate the cooperativity of weakly bound S1 along actin filaments. Thus, we measured the distance of the nearest-neighbor S1 on actin filaments and compared the distribution of this distance with a computer simulation. As a result, when a weakly bound S1 molecule was assumed to prohibit other S1 molecules from binding to the adjacent actin monomer by a factor of 1/2, the best fit was obtained. This decrease in affinity could be ascribed to steric hindrance of S1. We concluded that the weakly bound S1 shows no cooperativity in its binding along pure actin filaments in the presence of ATP and speculated that the cooperative binding of S1 molecules is not required for force generation in muscle contraction. Cooperativity of S1 binding along actin filaments in the presence of troponin and tropomyosin should be examined. Furthermore, our results suggest that S1 binding may not cause a long-range conformational change along pure actin filaments. Ménétret et al. (1991) reported a remarkable undulation of actin filaments during dissociation of S1 induced by photolysis of caged adenylimidodiphosphate (AMP-PNP). However we did not detect such a dynamic structural change of actin filaments in the presence of ATP.

In summary, using our newly developed freezing system coupled with the caged compound technique, we pursued the time course of the transition of acto-S1 complex from the strong to the weak binding state at the electron microscope level, and obtained simultaneous structural information of S1, actin, and their interaction. We believe further detailed analysis of the behavior of S1 in the presence of ATP, especially during sliding, using our freezing system will lead to a better understanding of the molecular mechanism of muscle contraction.

This freezing system is also highly applicable to the analysis of many intracellular events other than muscular contraction, since various caged compounds are now available (Gurney and Lester, 1987; McCray and Trentham, 1989; Kaplan, 1990).

We thank Dr. Keisuke Horiuti (Medical College of Oita, Oita, Japan) for his cooperation in making the ultraviolet light source and for his useful advice on experiments of photolysis. Our thanks are also due to Dr. Akihiko Ishijima (HONDA R&D Co. Ltd, Saitama, Japan), Mr. Tetsuichi Wazawa, and Mr. Yosuke Yasuda (Osaka University, Osaka, Japan) for their help in computer simulation experiments and data analyses of electron micrographs. We are also grateful to Drs. Shin'ichi Ishiwata (Waseda University, Tokyo, Japan) and Hideo Higuchi (Jikei University, Tokyo, Japan) for their critical reading of the manuscript. Our thanks are also due to Mr. Akio Ohba, Mr. Hiroshi Maebashi, and our laboratory staff (National Institute for Physiological Sciences, Aichi, Japan) for their technical assistance and helpful discussion.

This work was partially supported by a Grant-in-Aid for the encouragement of young scientist (to T. Funatsu) and for scientific research (to S. Tsukita) from the Ministry of Education, Science, and Culture of Japan.

Received for publication 14 January 1992 and in revised form 10 March 1993.

References

Ando, T., and D. Scales. 1985. Skeletal muscle myosin subfragment-1 induces bundle formation by actin filaments. *J. Biol. Chem.* 260:2321-2327.

Applegate, D., and P. Flicker. 1987. New states of actomyosin. *J. Biol. Chem.* 262:6856-6863.

Berger, C. L., E. C. Svensson, and D. D. Thomas. 1989. Photolysis of a photolabile precursor of ATP (caged ATP) induces microsecond rotational motions of myosin heads bound to actin. *Proc. Natl. Acad. Sci. USA.* 86:8753-8757.

Bradford, M. M. 1976. A rapid and sensitive method for the quantitation of microgram quantities of protein utilizing the principle of protein-dye binding. *Anal. Biochem.* 72:248-254.

Brenner, B., M. Schoenberg, J. M. Chalovich, L. E. Greene, and E. Eisenberg. 1982. Evidence for cross-bridge attachment in relaxed muscle at low ionic strength. *Proc. Natl. Acad. Sci. USA.* 79:7288-7291.

Brenner, B., L. C. Yu, and R. J. Podolsky. 1984. X-ray diffraction evidence for cross-bridge formation in relaxed muscle fibers at various ionic strengths. *Biophys. J.* 46:299-306.

Chalovich, J. M., and E. Eisenberg. 1981. Inhibition of actomyosin ATPase activity by troponin-tropomyosin without blocking the binding of myosin to actin. *J. Biol. Chem.* 257:2432-2437.

Craig, R., L. E. Greene, and E. Eisenberg. 1985. Structure of the Actin-myosin Complex in the Presence of ATP. *Proc. Natl. Acad. Sci. USA.* 82: 3247-3251.

Dantzig, J. A., M. G. Hibberd, D. R. Trentham, and Y. E. Goldman. 1991. Cross-bridge kinetics in the presence of MgADP investigated by photolysis of caged ATP in rabbit psoas muscle fibers. *J. Physiol.* 432:639-680.

Eisenberg, E., and T. L. Hill. 1985. Muscle contraction and free energy transduction in biological systems. *Science (Wash. DC).* 227:999-1006.

Frado, L.-L., and R. Craig. 1992. Electron microscopy of the actin-myosin head complex in the presence of ATP. *J. Mol. Biol.* 223:391-397.

Goldman, Y. E., M. G. Hibberd, and D. R. Trentham. 1984. Relaxation of rabbit psoas muscle fibers from rigor by photochemical generation of adenosin-5'-triphosphate. *J. Physiol.* 354:577-604.

Green, L. E., and E. Eisenberg. 1980. Dissociation of the actin · subfragment 1 complex by adenyl-5'-yl imidodiphosphate, ADP, and PPi. *J. Biol. Chem.* 255:543-548.

Greene, L. E., J. Sellers, E. Eisenberg, and R. S. Adelstein. 1983. Binding of gizzard smooth muscle myosin subfragment 1 to actin in the presence and absence of adenosin 5'-triphosphate. *Biochemistry.* 22:530-535.

Gurney, A. M., and H. A. Lester. 1987. Light-flash physiology with synthetic photosensitive compounds. *Physiol. Rev.* 67:583-617.

Hanson, J., and J. Lowy. 1963. The structure of F-actin and of actin filaments isolated from muscle. *J. Mol. Biol.* 6:46-60.

Haselgrove, J. C., and H. E. Huxley. 1973. X-ray evidence for radial cross-bridge movement and for the sliding filament model in actively contracting skeletal muscle. *J. Mol. Biol.* 77:549-568.

Heuser, J. E., T. S. Reese, M. J. Dennis, Y. Jan, L. Jan, and L. Evans. 1979. Synaptic vesicle exocytosis captured by quick freezing and correlated with quantal transmitter release. *J. Cell Biol.* 81:275-300.

Heuser, J. E., and M. W. Kirschner. 1980. Filament organization revealed in platinum replicas of freeze-dried cytoskeletons. *J. Cell Biol.* 86:212-234.

Heuser, J. E. 1981. Preparing biological samples for stereomicroscopy by the quick-freeze, deep-etch, rotary-replication technique. *In* Methods in Cell Biology. J. Turner, editor. Academic Press, New York. 22:97-122.

Heuser, J. E., and R. Cooke. 1983. Actin-myosin interactions visualized by the quick-freeze, deep-etch replica technique. *J. Mol. Biol.* 169:97-122.

Horiuti, K., T. Sakoda, M. Takei, and K. Yamada. 1992. Effects of ethylene glycol on the kinetics of contraction upon flash photolysis of caged ATP in rat psoas muscle fibers. *J. Musc. Res. Cell Motil.* 13:199-205.

Huxley, H. E., and M. J. Kress. 1985. Crossbridge behavior during muscle contraction. *J. Musc. Res. Cell Motil.* 6:153-161.

Kaplan, J. H. 1990. Special topic: caged compounds in cellular physiology. *Annu. Rev. Physiol.* 52:853-855.

Katayama, E. 1989. The effects of various nucleotides on the structure of actin-attached myosin subfragment-1 studied by quick-freeze deep-etch electron microscopy. *J. Biochem. (Tokyo).* 106:751-770.

Katoh, T., and F. Morita. 1984. Interaction between myosin and F-actin. Correlation with actin-binding sites on subfragment-1. *J. Biochem. (Tokyo).* 96:1223-1230.

Lowy, J., and F. R. Poulsen. 1987. X-ray study of myosin heads in contracting frog skeletal muscle. *J. Mol. Biol.* 194:595-600.

Matsuda, T., and R. J. Podolsky. 1984. X-ray evidence for two structural states of the actomyosin cross-bridge in muscle fibers. *Proc. Natl. Acad. Sci. USA.* 81:2364-2368.

McCray, J. A., L. Herbette, T. Kihara, and D. R. Trentham. 1980. A new approach to time-resolved studies of ATP-requiring biological systems: laser flash photolysis of caged ATP. *Proc. Natl. Acad. Sci. USA.* 77:7237-7241.

McCray, J. A., and D. R. Trentham. 1989. Properties and uses of photoreactive caged compounds. *Annu. Rev. Biophys. Biophys. Chem.* 18:239-270.

Ménétret, J.-F., W. Hofmann, R. R. Schröder, G. Rapp, and R. S. Goody. 1991. Time-resolved cryo-electron microscopic study of the dissociation of actomyosin induced by photolysis of photolabile nucleotides. *J. Mol. Biol.* 219:139-144.

Pollard, T. D., P. Maupin, J. Sinard, and H. E. Huxley. 1990. A stopped-flow/rapid-freezing machine with millisecond time resolution to prepare intermediates in biochemical reactions for electron microscopy. *J. Electron Microsc. Tech.* 16:160-166.

Rosenfeld, S. S., and E. W. Taylor. 1984. The ATPase mechanism of skeletal and smooth muscle acto-subfragment 1. *J. Biol. Chem.* 259:11908-11919.

Siemankowski, R. F., M. O. Wiseman, and H. D. White. 1985. ADP dissociation from actomyosin subfragment 1 is sufficiently slow to limit the unloaded shortening velocity in vertebrate muscle. *Proc. Natl. Acad. Sci. USA.* 82:658-662.

Spudich, J. A., and S. Watt. 1971. The regulation of rabbi skeletal muscle contraction. *J. Biol. Chem.* 246:4866-4871.

Stein, L. A., R. Schwarz, P. B. Chock, and E. Eisenberg. 1979. Mechanism of actomyosin adenosine triphosphatase. Evidence that adenosine 5'-triphosphate hydrolysis can occur without dissociation of the actomyosin complex. *Biochemistry.* 18:3895-3909.

Trybus, K. M., and E. W. Taylor. 1980. Kinetic studies of the cooperative binding of subfragment 1 to regulated actin. *Proc. Natl. Acad. Sci. USA.* 77: 7209-7213.

Tsukita, S., and M. Yano. 1985. Actomyosin structure in contracting muscle detected by rapid freezing. *Nature (Lond.).* 317:182-184.

Tsukita, S., and M. Yano. 1988. Instantaneous view of actomyosin structure in shortening muscle. *In* Molecular Mechanism of Muscle Contraction. H. Sugi and G. H. Pollack, editors. Plenum Press, New York and London. 31-38.

Wakabayashi, K., M. Tokunaga, I. Kohno, Y. Sugimoto, T. Hamanaka, Y. Takezawa, T. Wakabayashi, and Y. Amemiya. 1992. Small-angle synchroton X-ray scattering reveals distinct shape change of the myosin head during hydrolysis of ATP. *Science (Wash. DC).* 258:443-447.

Weeds, A. G., and R. S. Taylor. 1975. Separation of subfragment-1 isoenzymes from rabbit skeletal muscle myosin. *Nature (Lond.).* 257:54-56.

White, H. D., and E. W. Taylor. 1976. Energetics and mechanism of actomyosin adenosine triphosphate. *Biochemistry.* 15:5818-5826.